Supporting Information

$CoFe_2O_4$ Hollow Spheres Decorated Three-Dimensional rGO Sponge for Highly Efficient Electrochemical Charge Storage Device

Debika Gogoi,[a] *Manash R. Das,*[bc] *Narendra Nath Ghosh*[a]*

[a] Nano-materials Lab, Department of Chemistry, Birla Institute of Technology and Science, Pilani K K Birla Goa Campus, Zuarinagar 403726, Goa, India.

[b] Advanced Materials Group, Materials Sciences and Technology Division, CSIR-North East Institute of Science and Technology, Jorhat 785006, Assam, India.

[c] Academy of Scientific and Innovative Research (AcSIR), Ghaziabad 201002, India.

*Corresponding author. Tel. /fax: +91 832 2580318/25570339.
*E-mail address: naren70@yahoo.com (N. N. Ghosh)
Author's email addresses: p20180429@goa.bits-pilani.ac.in (Debika Gogoi), mnshrdas@yahoo.com (Manash R. Das)

S1. Materials Synthesis

S1.1. Chemicals used. Cobalt chloride hexahydrate ($CoCl_2.6H_2O$), Ferric chloride hexahydrate ($FeCl_3.6H_2O$), and ethylene glycol were purchased from Merck, India. Polyethylene glycol (PEG-2000), Sodium hydroxide (NaOH), Hydrazine hydrate, Sulphuric acid (H_2SO_4), Potassium Hydroxide (KOH), Methanol (HPLC grade) and ethanol were purchased from Fisher Scientific. Graphite powder (mean particle size of <20 mm), Polyvinylidene difluoride (PVDF), acetylene black, N-methyl-2-pyrrolidinone (NMP) and polyvinyl alcohol (PVA) were purchased from Sigma-Aldrich. All the chemicals were used without further purification. Deionized water was used throughout the experiment.

S1.2. Synthesis of Graphene oxide (GO)

GO was synthesized by using modified Hummer's method. In the standard synthetic process, 0.6 g $NaNO_3$ was added to 35 mL conc. H_2SO_4 taken in a beaker kept inside an ice-bath. Then 1.3 g of graphite powders were added to the mixture and stirred for 8 h by maintaining the temperature below 5^oC. To this mixture, 3.8 g of $KMnO_4$ was added slowly and the temperature of the mixture was raised to ~35^oC and stirred for 8-10 h. Then 180 mL of distilled water was added to the mixture and the temperature was raised to 98^oC and maintained for ~1 h. After that 2 mL of 30% H_2O_2 solution was added to the mixture and stirred for 1 h. The obtained product (GO) was washed with 10% HCl solution, distilled water and ethanol and then dried at 60^oC for 10 h.

S1.3. Synthesis of reduced graphene oxide (rGO) with nanosheet-like structure

1 g of GO was dispersed in 200 mL distilled water and then 2 M NaOH was added drop by drop to this mixture till pH reaches ~12. The mixture was stirred for ~30 min and then 56 mL of hydrazine hydrate was added and refluxed for 4 h. The black ppt. obtained was washed with distilled water till pH of the mixture reaches ~7 followed by washing with ethanol and finally dried at 60^oC for 10 h.

S1.4. Preparation of GO sponge (GO_{sp}) and rGO sponge (rGO_{sp})

In a beaker, GO was well-dispersed in minimum amount of water and then kept in -80^oC for overnight followed by lyophilisation for 72 h. The obtained GO sponge was the kept in vacuum oven at 60^oC for 10h. The prepared GO_{sp} was placed in an alumina crucible and 6

mL hydrazine hydrate and then the crucible was covered with a lid. Then it was heated for 3 h at 150^{o}C to obtain rGO_{sp}.

S1.5. Synthesis of $CoFe_2O_4$ hollow spheres (CF_{hs})

In a beaker $CoCl_2.6H_2O$ and $FeCl_3.6H_2O$ (molar ratio=1:2) were dissolved in 80 ml of ethylene glycol. To this mixture sodium acetate and poly ethylene glycol-2000 (PEG-2000) (weight ratio 1:3.6) were added and then stirred vigorously until NaAc and PEG-2000 gets completely dissolved. The mixture was then transferred to a stainless steel autoclave and heated at 200^{o}C for 22 h. The obtained ppt. was separated from the reaction mixture by using an external magnet followed by washing with distilled water and ethanol and then dried at 60^{o}C for 10 h**.**

S1.6. Synthesis of CF_{hs}-rGO_{sp} nanocomposites

CF_{hs}-rGO_{sp} nanocomposites were prepared by employing a simple wet-impregnation method. In a round bottom flask, desired amount of CF_{hs} and rGO_{sp} were dispersed in methanol and the refluxed for 3 h and then the obtained product was separated from the solvent by using an external magnet and then dried at 60^{o}C for 10 h, for further use.

S2. Characterization and Instrumentation. For this work, we have used an Alpha 1-2 LD plus freeze dryer (Martin Christ, Germany) to prepare the GO sponge. Then, characterization of the synthesized materials were carried out by using the following characterization techniques: (i) X-ray diffraction (XRD) patterns were recorded using a powder X-ray diffractometer (Mini Flex II, Rigaku, Japan) with Cu Kα (λ = 0.15405 nm) radiation at a scanning speed of 3 $^{\circ}$ min^{-1}, (ii) Field emission scanning electron microscopy (FESEM) images of samples were obtained using Quanta 250 FEG (FEI), (iii) High-resolution transmission electron microscopy (HRTEM) and selected area electron diffraction (SAED) images were obtained by JEM-2100 (JEOL), 200 kV equipped with LaB_6 filament, (iv) Energy dispersive X-ray spectra (EDS) and elemental mapping of the synthesized material was obtained from X-Max (Oxford Instruments) attached to a JEOL JEM 2100 TEM operated at 200 kV, (v) Fourier Transform Infrared spectra (FTIR) were recorded using Spectrum two FT-IR spectrometer (Perkin Elmer), (vi) Raman spectra were recorded on a Horiba via Raman microscope with a 633 nm laser excitation, (vii) XPS measurements were carried out by using a Thermo-Scientific ESCALAB Xi^{+} spectrometer having a monochromatic Al Kα X-ray source (1486.6 eV) and a spherical energy analyzer that

operates in the CAE (constant analyzer energy) mode. (vii) Multiple point BET surface area was determined by a Surface area and porosimetry analyzer (Micromeritics Tristar 3000, USA).

IVIUMSTAT (10V/5A/8MHz) workstation was used to perform the electrochemical studies.

S3. Electrode preparation:

To fabricate the working electrode, first, a viscous paste of 80 wt % active electrode material with 10 wt % poly(vinylidene fluoride) in N-methyl-2-pyrrolidinone and 10 wt % acetylene black was prepared and then this paste was coated on the nickel foam with deimensions (1.5 cm × 1.5 cm) and dried at 80 $^{\circ}$C for 24 h under vacuum to remove the residual solvent. Mass loading on the Ni foam was ~2 mg.

Only one side of the Ni foam was coated in case of the working electrode for asymmetric cell.

S4. Fabrication of an asymmetric supercapacitor (ASC) cell.

The voltammetric charges (Q) were calculated based on the following equations:

$$Q = C_{single} \times \Delta V \times m \qquad \text{(S1)}$$

where m is the mass of the electrode (g), ΔV is the potential window (V), and C_{single} is the specific capacitance (F g^{-1}) of each electrode measured in three-electrode setup (calculated from cyclic voltammograms at a scan rate of 10 mV s^{-1}).

Considering the charge/mass ratio for both anode and cathode, balancing of charge was carried out by substituting above equation as:

$$\frac{q+}{q_-} = \frac{m+}{m_-} = \frac{C_{sp}{}^{-} \times \Delta V^{-}}{C_{sp}{}^{+} \times \Delta V+} \qquad \text{(S2)}$$

Where C_{sp^-} is the C_S value obtained for the anode material in the potential window ΔV^{-}, C_{sp^+} is the C_S value obtained for the cathode material in the potential window ΔV^{+}.

S5. Fabrication of the flexible supercapacitor device.

30 mL distilled water was taken in a beaker and heated on a hotplate. 1.6 g KOH was added to the boiling water followed by the addition of 0.42 g $K_4[Fe(CN)_6]$. Then 3.2 g of PVA was

added gradually to the reaction mixture and stirred till a thick gel was formed. This gel was then pasted between the positive and negative electrode and allowed to cool and dried at room temperature for overnight.

S6. Equations used:

The values of specific capacitance (C_s) for the three-electrode cell and the two-electrode asymmetric cells were calculated by using the following equation:

$$C_s = \frac{i\Delta t}{m\Delta V} \quad \text{(S3)}$$

Where, i represents the charge or discharge current in Ampere (A), Δt is the discharge time in seconds (s), m represents the mass of supercapacitive material in gram (g) and ΔV is the applied potential window.

For the two-electrode asymmetric cell, the energy density (E), the power density (P), and the Coulombic efficiency (η) were determined by using the following equations:

$$E = \frac{C_s \times (\Delta V)^2}{2} \quad \text{(S4)}$$

$$P = \frac{E}{\Delta t} \quad \text{(S5)}$$

$$\eta(\%) = t_d/t_c \times 100 \quad \text{(S6)}$$

where, t_d is the discharging time, t_c is the charging time.

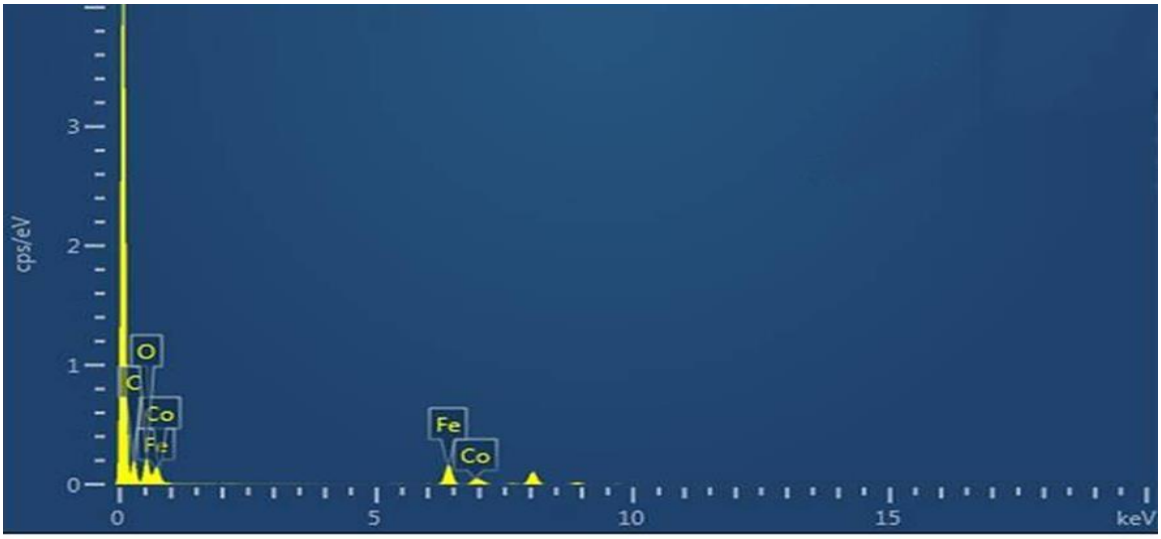

Figure S1. EDS spectra of 80CF_{hs}-20rGO_{sp}

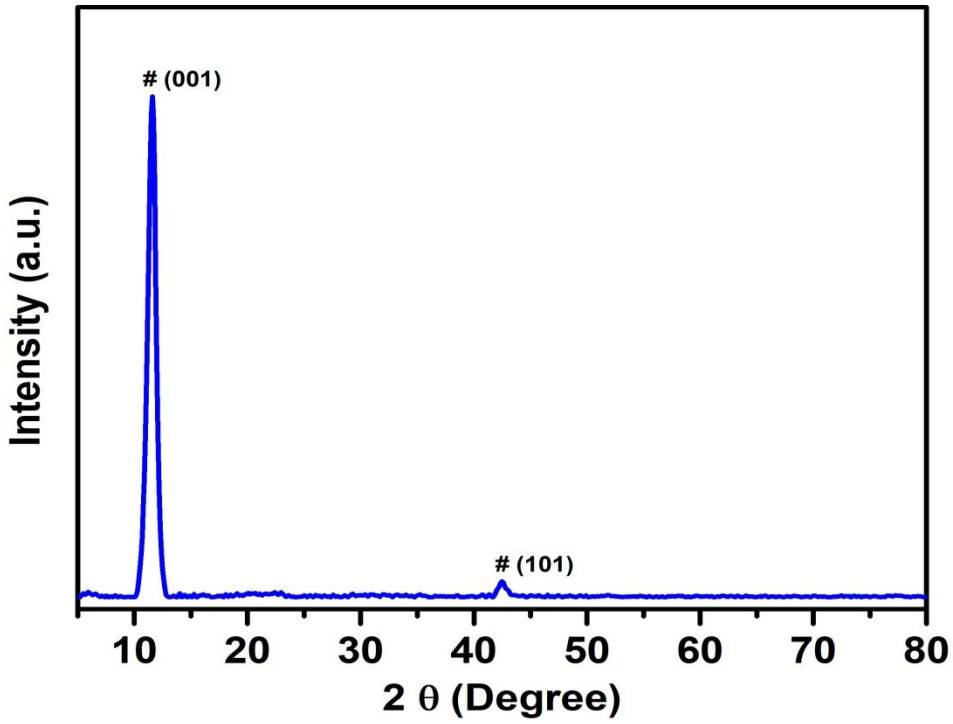

Figure S2. XRD of Graphene oxide (GO)

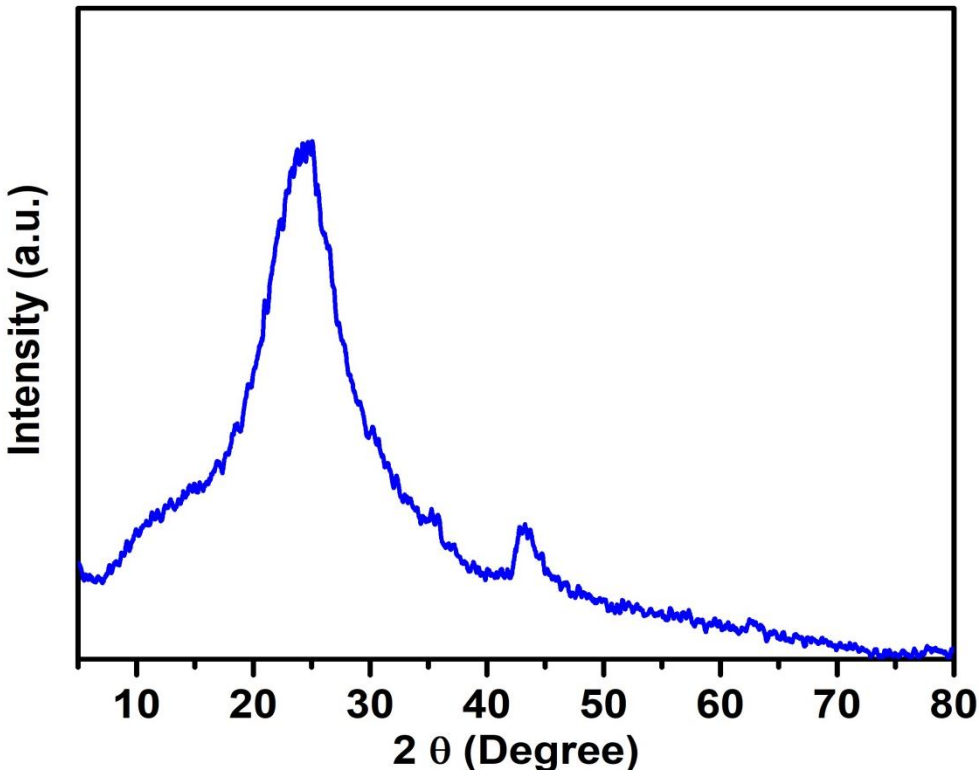

Figure S3. XRD of rGO nanosheets

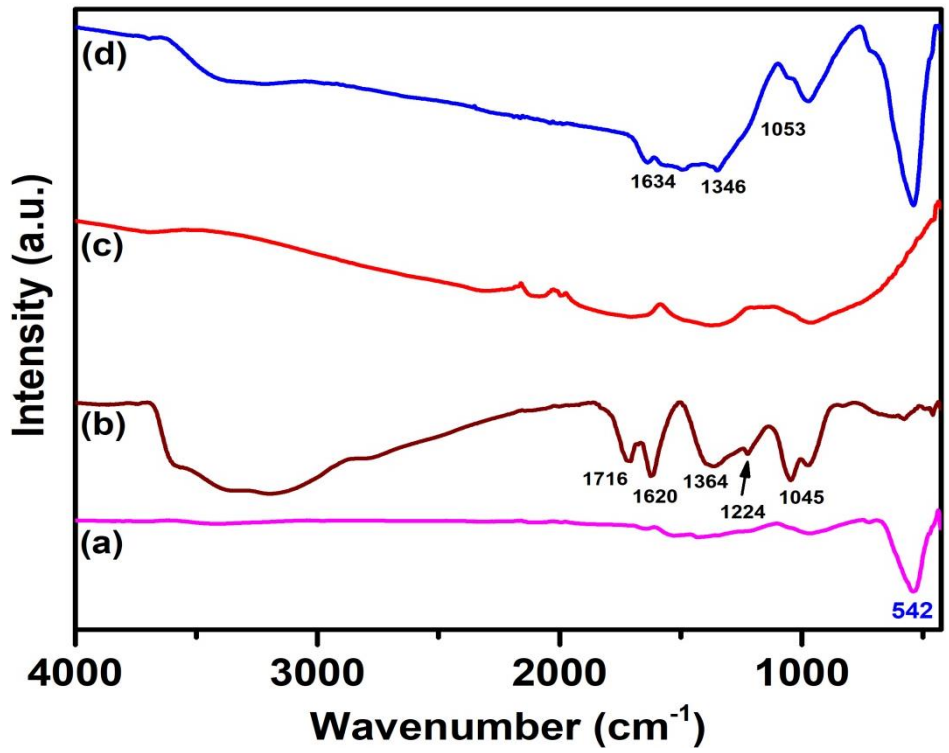

Figure S4. FTIR spectra of (a) CF_{hs}, (b) GO_{sp}, (c) rGO_{sp}, and (d) $80CF_{hs}$-$20rGO_{sp}$

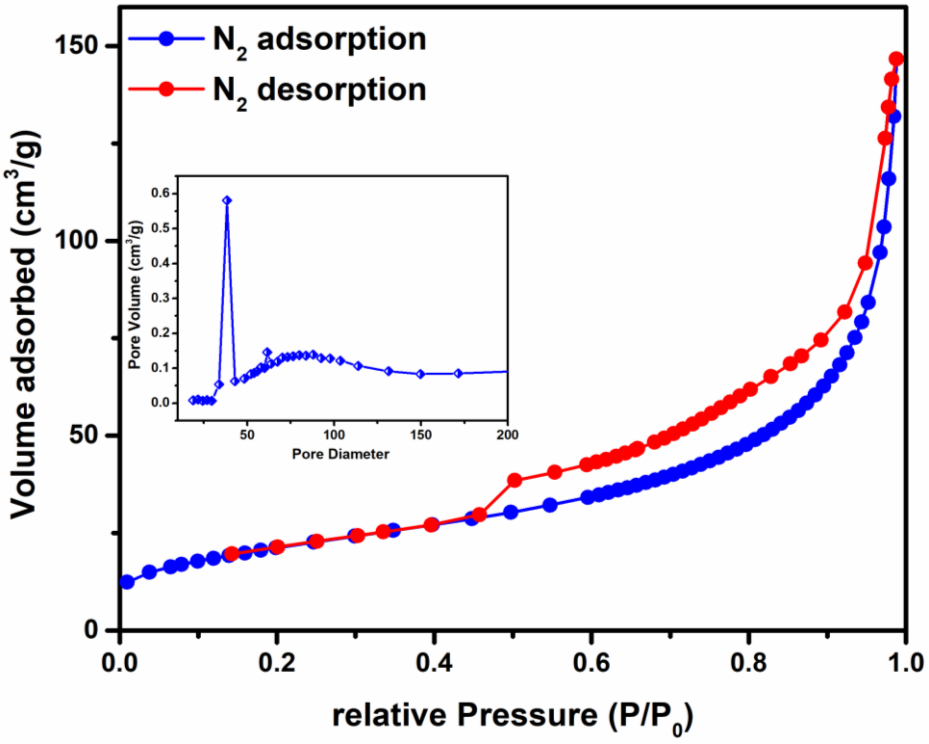

Figure S5. N_2 adsorption-desorption isotherm, inset: pore size distribution of $80CF_{hs}$-$20rGO_{sp}$ nanocomposite.

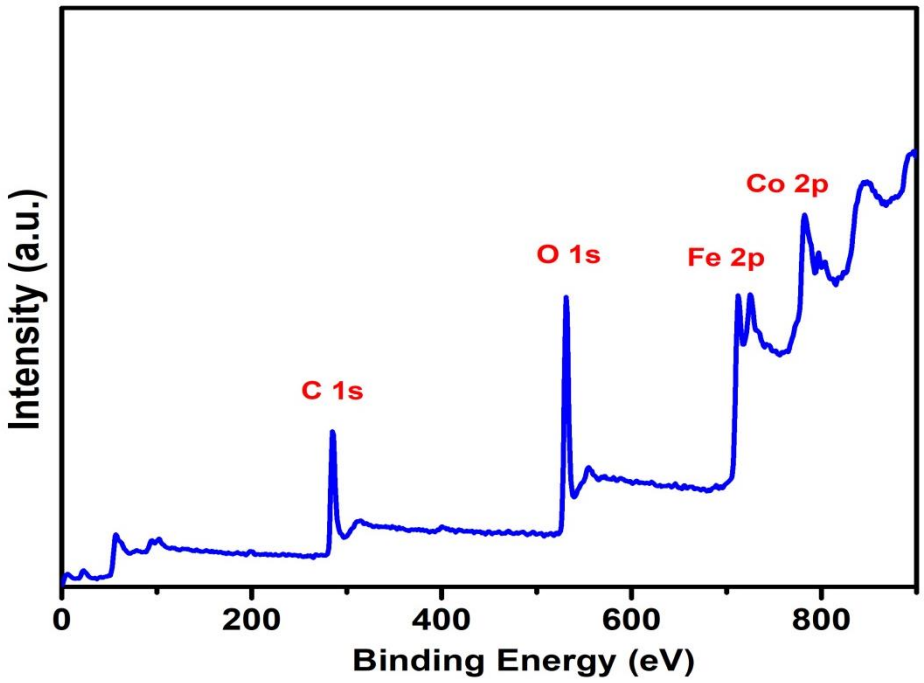

Figure S6. XPS survey spectrum of $80CF_{hs}$-$20rGO_{sp}$

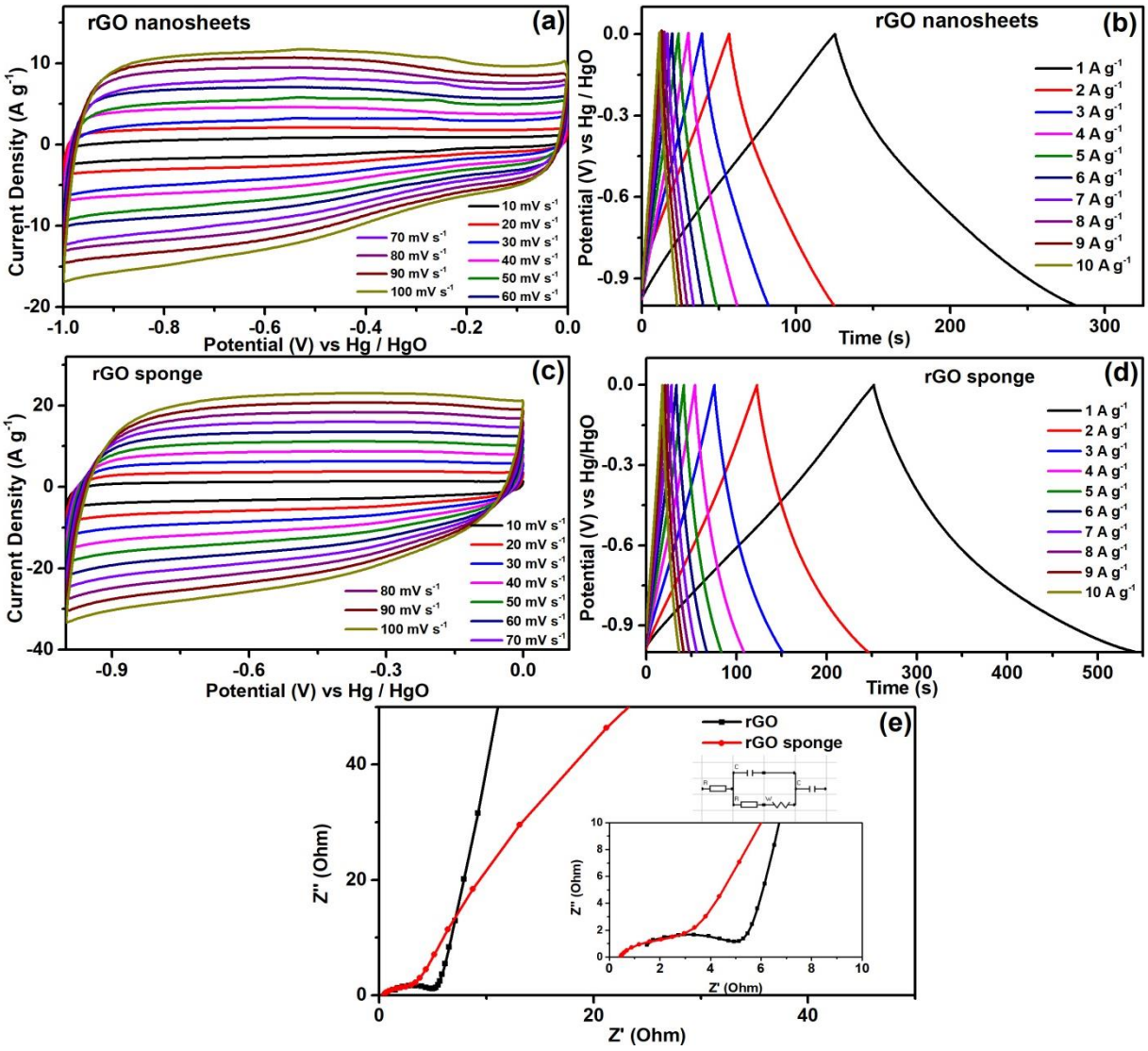

Figure S7. CV profiles at various scan rates and GCD curves at various current densities of (a), (b) rGO nanosheet; (c), (d) rGO sponge; and (e) Nyquist plots of rGO nanosheets and rGO sponge, inset shows the equivalent circuit used for fitting the Nyquist plots and the EIS curves at high frequency region.

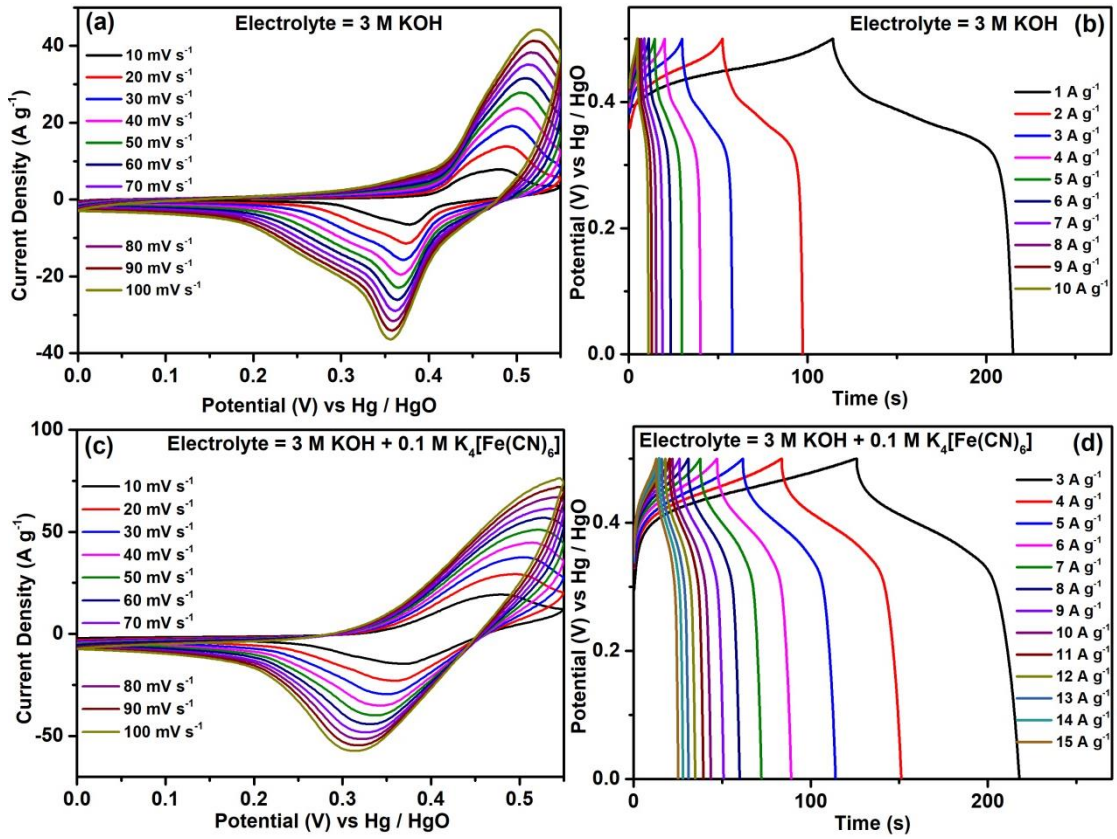

Figure S8. CV profiles at various scan rates and GCD curves at various current densities of CF_{hs} in (a), (b) 3 M KOH electrolyte; (c), (d) 3 M KOH + 0.1 M $K_4[Fe(CN)_6]$ electrolyte.

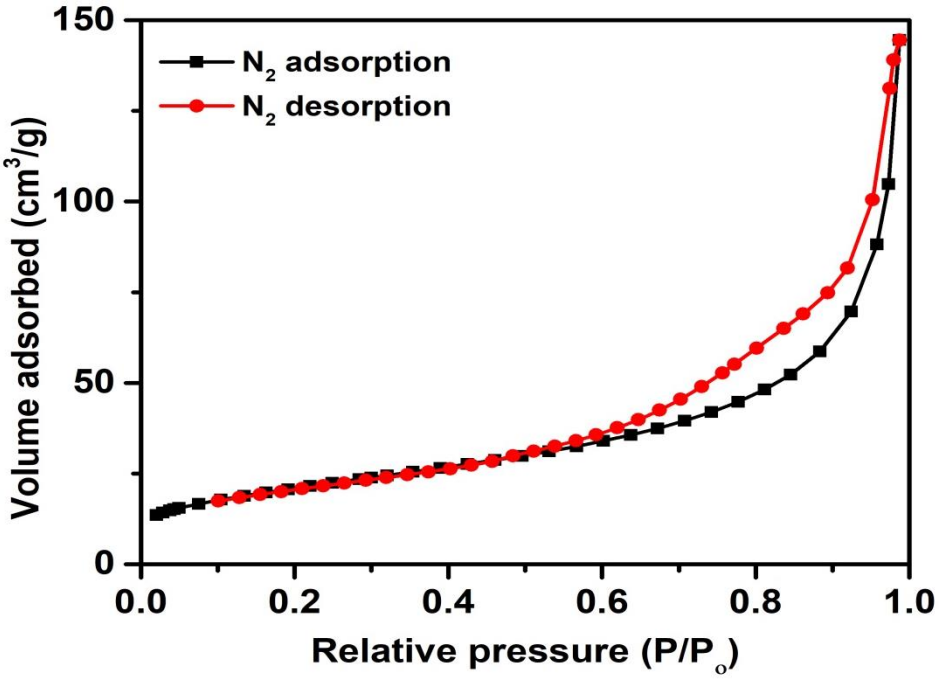

Figure S9. N2 adsorption-desorption isotherm of CF_{hs}.

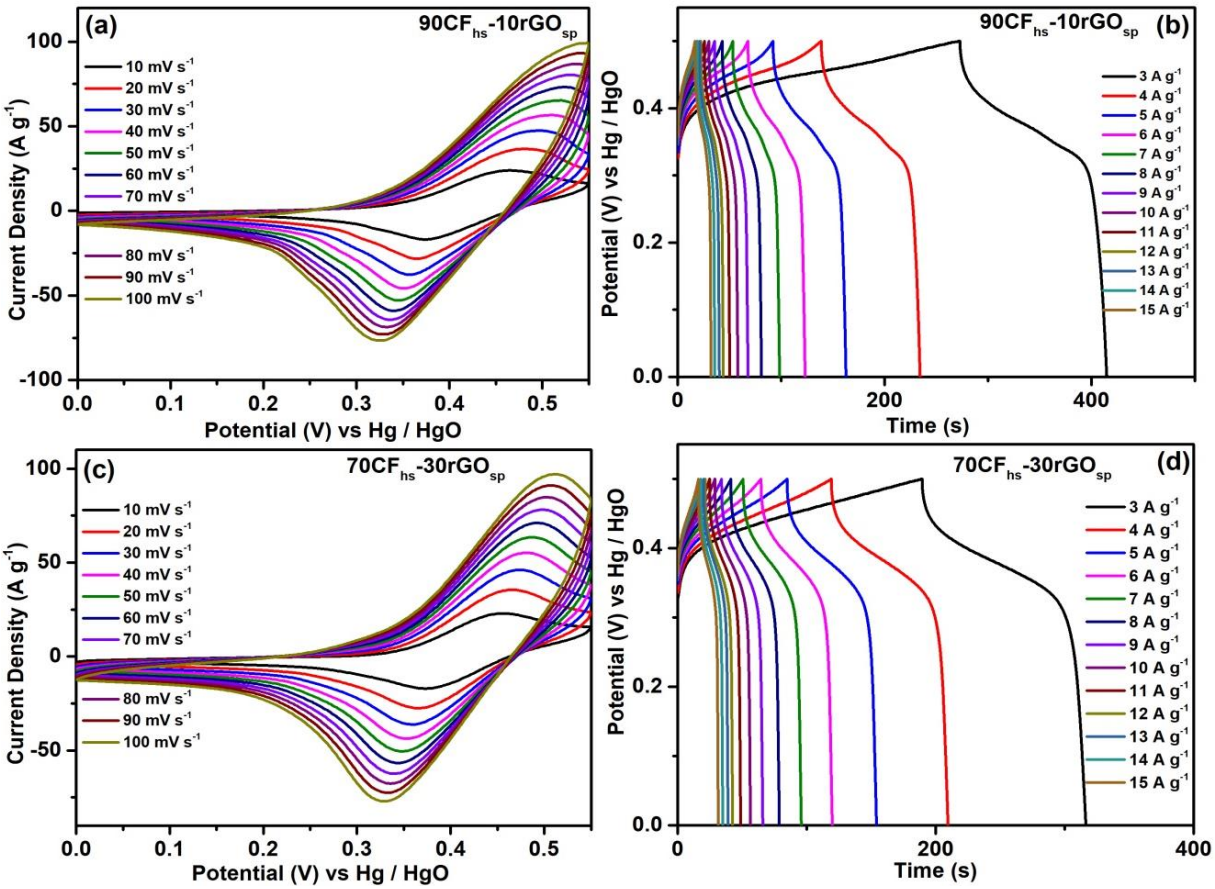

Figure S10. CV curves at different scan rates and GCD curves at different current densities of (a), (b) $90CF_{hs}$-$10rGO_{sp}$, and (c), (d) $70CF_{hs}$-$30rGO_{sp}$.

Table S1. Obtained EIS data of the electrode materials after circuit fitting

S. No.	Material	Equivalent Series Resistance (R_1=R_S) Ω	Charge Transfer Resistance (R_2=R_{CT}) Ω	Warburg Resistance (W) Ω	C_1=C_{DL} (F)	C_2=C_L (F)
1	Pure CF (in 3 M KOH)	0.45	19.3	1.66E-03	3.03E-03	8.34E+00
2	Pure CF (in 3M KOH+ 0.1M $K_4[Fe(CN)_6]$	0.44	9.2	1.69E-03	3.04E-03	1.00E+01
3	Pure rGO	1.39	3.68	6.52E-01	2.22E-03	1.91E-01
4	rGO sponge	0.68	2.33	2.34E-02	1.76E-01	3.30E-01
5	90CF-10rGO sponge	0.38	0.53	4.34E-02	9.38E-04	7.01E-02
6	80CF-20rGO sponge	0.37	0.38	1.18E-02	1.92E-02	3.89E-01
7	70CF-30rGO sponge	0.47	0.77	3.79E-02	9.52E-04	4.29E-01

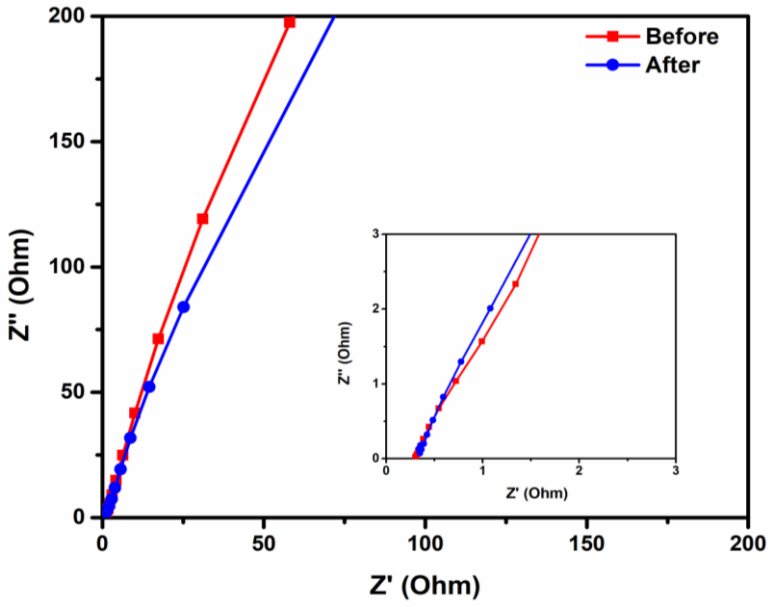

Figure S11. Nyquist plot of $80CF_{hs}$-$20rGO_{sp}$ before and after ~5000 GCD cycles.

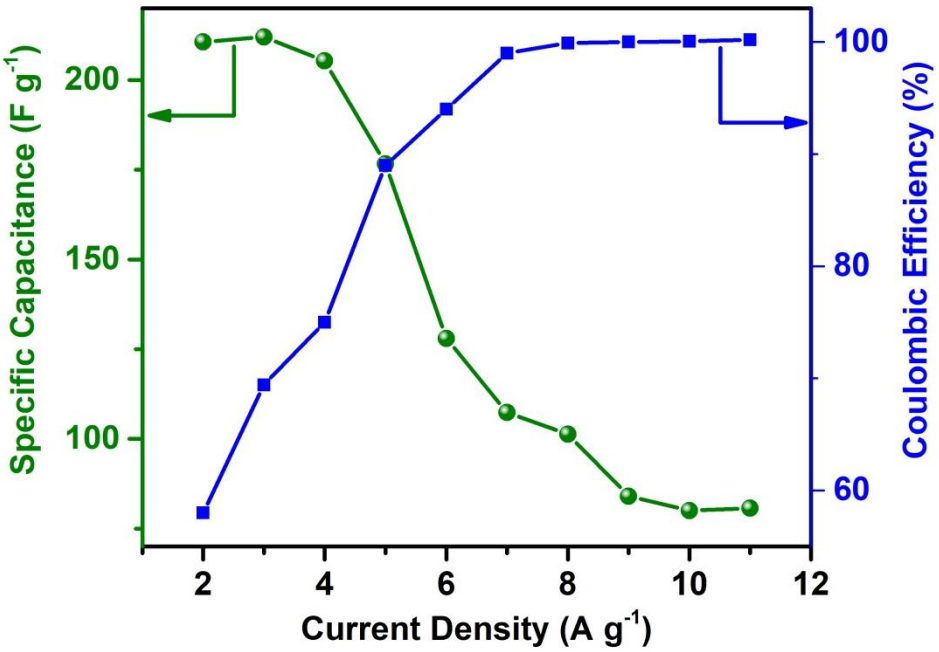

Figure S12. Variation of specific capacitance and Coulombic efficiency with current density.

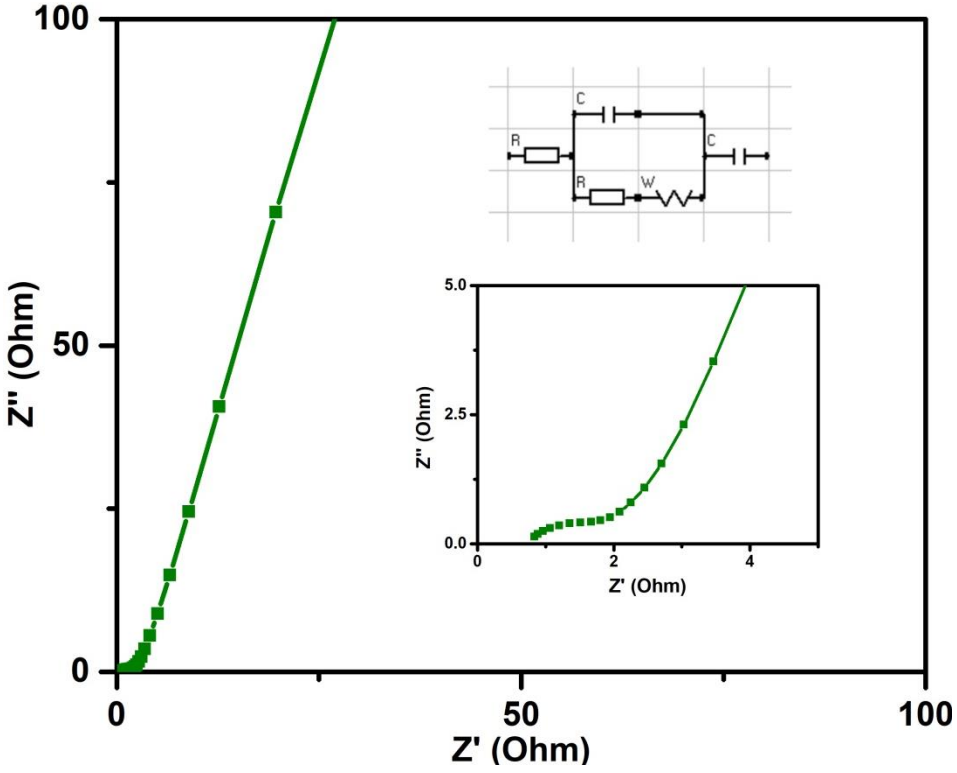

Figure S13. Nyquist plot of the fabricated all-solid-state flexible supercapacitor device.

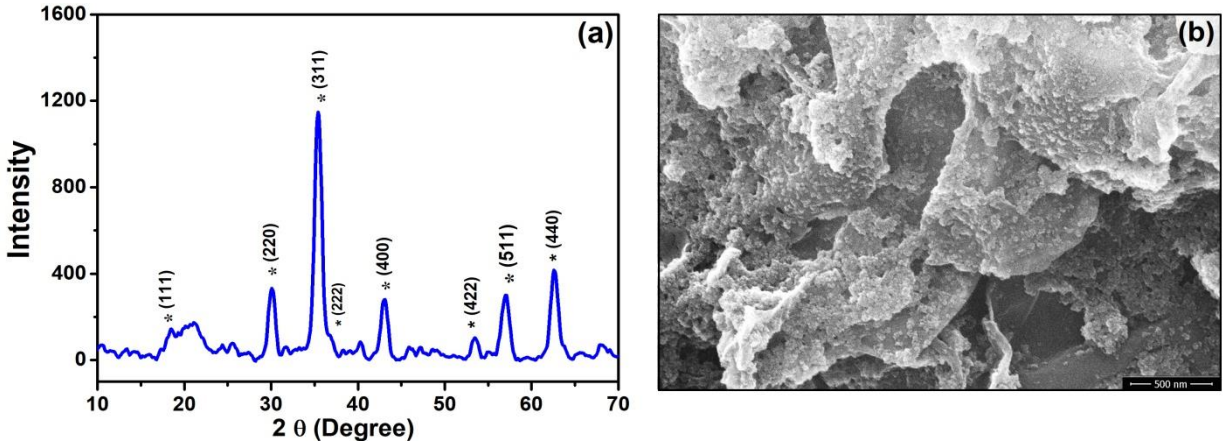

Figure S14. (a) XRD patterns (b) FESEM micrograph of used $80CF_{hs}$-$20rGO_{sp}$ nanocomposite.

Table S2. Comparison table of the fabricated flexible ASC device (this work) with some of the already reported carbon-based two-electrode asymmetric supercapacitors.

S. No.	Material	Electrolyte	Working Potential (V)	Power Density (W kg^{-1})	Energy Density (W h kg^{-1})	Retention	Ref.
1.	$CoFe_2O_4$/rGO‖ rGO hydrogel	6 M KOH	0-1.3	650	17.84	87% (4000 cycles)	1
2.	$CoFe_2O_4$‖graphene	1 M KOH	0-1.5	643	12.14	67% (3000 cycles)	2
3.	CoFe2O4/rGO‖ Fe3O4/rGO	1 M KOH	0-1.7	840	45.5	91% (5000 cycles)	3
4.	$Co_{1-x}S$/CoFe2O4@rGO‖AC	2 M KOH	0-1.4	700	61.5	84% (10000 cycles)	4
5.	NS/CoFe2O4/CoOOH‖rGO/PEDOT:PSS	3 M KOH	0-1.6	374.9	54.1	-	5
6.	Carbon spheres/MnO_2‖ Carbon spheres	0.1 M Na_2SO_4	0-2	100	22.1	99% (1000 cycles)	6

7.	NiS‖CNFs	2 M KOH	0-1.55	387.5	34.9	90.2% (3000 cycles)	7
8.	Co_3O_4 NSs-rGO ‖ AC	2 M KOH	0-1.45	2166	13.4	89% (1000 cycles	8
9.	Co_3O_4@CoNiS‖ NOPC	3 M KOH	0-1.6	400	46.95	95.6% (20000 cycles)	9
10.	CuO‖AC	3 M KOH	0-1.4	700	19.7	96% (3000 cycles)	10
11.	NiS‖AC	3 M KOH	0-1.8	900	31	100% (1000 cycles)	11
12.	MnO_2‖Graphene hydrogel	0.1 M Na_2SO_4	0-2	1000	23.2	83.4% (5000 cycles)	12
13.	CNTG-40‖MG-50	PAAK/KCl	0-1.8	9000	32.7 (22.9)	86% (10000 cycles	13
14.	AC‖δ-ACEP@MnO_2	1 M Na_2SO_4	0-2	500	31	92.8% (5000 cycles)	14
15.	MnO_2/GPCN-SS‖GPCN-SS	1 M Na_2SO_4	0-2	516	50.2	99.1% (10000 cycles)	15
16.	NCS-650‖AC	6 M KOH	0-1.2	331	10.3	88% (5000 cycles)	16
17.	NiCoP nanoplates‖ graphene films	1 M KOH + Porous polymer membrane (Celgrade 3501)	0-1.5	1301	32.9	83.1 % (5000 cycles)	17
18.	CF-200‖ LRGONR	PVA/KOH	0-1.6	727.8	33.5	95.8% (5000 cycles)	18
19.	L-$CoFe_2O_4$/C ‖AC	2 M KOH	0-1.6	720	14.38	76.6 (800 cycles)	19
20.	$CoFe_2O_4$/CNT‖ AC	2 M KOH	0-1.6	400	30.4	85.6% (1000 cycles)	20

21.	NFO/GNSs-10 ‖AC	6 M KOH	0-1.5	70	14.01	140% (5000 cycles)	21
22.	CC/ZnO@C@ NiO‖graphene	3 M KOH + PVA	0-1.4	380.9	35.7	87% (10000 cycles)	22
23.	$80MnFe_2O_4$-20rGO‖rGO	3 M KOH + 0.1 M $K_4[Fe(CN)_6]$	0-1.5	750	27.7	95% (4000 cycles)	23
24.	$(Ag_{0.50}Ni_{0.50})_{90}$-$rGO_{10}$‖rGO	3 M KOH	0-1.7	1700	49	97% (5000 cycles)	24
25	$CuFe_2O_4$-rGO||rGO	3 M KOH + 0.1 M $K_4[Fe(CN)_6]$ in PVA	0-1.3	2600	38	97% (10,000 cycles)	25
26	$(CoNi_D)_{60}$-rGO_{40}||rGO	3 M KOH + 0.1 M $K_4[Fe(CN)_6]$ in PVA	0-1.6	2000	52.8	95% (4000 cycles)	26
27.	$80CF_{hs}$-$20rGO_{sp}$‖rGO_{sp}	3 M KOH + 0.1 M $K_4[Fe(CN)_6]$ in PVA	0-1.5	1500	65.8	96% (5000 cycles)	**This Work**

References

1. Zheng, L.; Guan, L.; Yang, G.; Chen, S.; Zheng, H. One-pot synthesis of $CoFe_2O_4$/rGO hybrid hydrogels with 3D networks for high capacity electrochemical energy storage devices. *RSC Adv.* **2018**, *8*, 8607-8614.

2. Sankar, K. V.; Selvan, R. K.; Meyrick, D. Electrochemical performances of $CoFe_2O_4$ nanoparticles and a rGO based asymmetric supercapacitor. *RSC Adv.* **2015**, *5*, 99959-99967.

3. Wang, H.; Song, Y.; Ye, X.; Wang, H.; Liu, W.; Yan, L. Asymmetric supercapacitors assembled by dual spinel ferrites@graphene nanocomposites as electrodes. *ACS Appl. Energy Mater*. **2018**, *1*, 3206-3215.

4. Ren, C.; Jia, X.; Zhang, W.; Hou, D.; Xia, Z.; Huang, D.; Hu, J.; Chen, S.; Gao, S. Hierarchical Porous Integrated $Co_{1-x}S/CoFe_2O_4$@rGO Nanoflowers Fabricated via Temperature-Controlled In Situ Calcining Sulfurization of Multivariate CoFe-MOF-74@ rGO for High-Performance Supercapacitor. *Adv. Funct. Mater.* **2020**, *30*, 2004519.

5. Song, K.; Wang, X.; Li, J.; Zhang, B.; Yang, R.; Liu, P.; Wang, J. 3D hierarchical $CoFe_2O_4$/CoOOH nanowire arrays on Ni-Sponge for high-performance flexible supercapacitors. *Electrochim. Acta* **2020**, *340*, 135892.

6. Lei, Z.; Zhang, J.; Zhao, X. S. Ultrathin MnO_2 nanofibers grown on graphitic carbon spheres as high-performance asymmetric supercapacitor electrodes. *J. Mater. Chem.* **2012**, *22*, 153-160.

7. Ma, X.; Zhang, L.; Xu, G.; Zhang, C.; Song, H.; He, Y.; Zhang, C.; Jia, D. Facile synthesis of NiS hierarchical hollow cubes via Ni formate frameworks for high performance supercapacitors. *Chem. Eng. J.* **2017**, *320*, 22-28.

8. Yuan, C.; Zhang, L.; Hou, L.; Pang, G.; Oh, W.-C. One-step hydrothermal fabrication of strongly coupled Co_3O_4 nanosheets–reduced graphene oxide for electrochemical capacitors. *RSC Adv.* **2014**, *4*, 14408-14413.

9. Yan, Y.; Ding, S.; Zhou, X.; Hu, Q.; Feng, Y.; Zheng, Q.; Lin, D.; Wei, X. Controllable preparation of core-shell Co_3O_4@CoNiS nanowires for ultra-long life asymmetric supercapacitors. *J. Alloys Compd.* **2021**, *867*, 158941.

10. Moosavifard, S. E.; El-Kady, M. F.; Rahmanifar, M. S.; Kaner, R. B.; Mousavi, M. F. Designing 3D highly ordered nanoporous CuO electrodes for high-performance asymmetric supercapacitors. *ACS Appl. Mater. Interfaces* **2015**, *7*, 4851-4860.

11. Guan, B.; Li, Y.; Yin, B.; Liu, K.; Wang, D.; Zhang, H.; Cheng, C. Synthesis of hierarchical NiS microflowers for high performance asymmetric supercapacitor. *Chem. Eng. J.* **2017**, *308*, 1165-1173.

12. Gao, H.; Xiao, F.; Ching, C. B.; Duan, H. High-performance asymmetric supercapacitor based on graphene hydrogel and nanostructured MnO_2. *ACS Appl. Mater. Interfaces* **2012**, *4*, 2801-2810.

13. Gao, H.; Xiao, F.; Ching, C. B.; Duan, H. Flexible All-Solid-State Asymmetric Supercapacitors Based on Free-Standing Carbon Nanotube/Graphene and Mn_3O_4 Nanoparticle/Graphene Paper Electrodes. *ACS Appl. Mater. Interfaces* **2012**, *4*, 7020-7026.

14. Wang, X.; Chen, S.; Li, D.; Sun, S.; Peng, Z.; Komarneni, S.; Yang, D. Direct Interfacial Growth of MnO_2 Nanostructure on Hierarchically Porous Carbon for High-Performance Asymmetric Supercapacitors. *ACS Sustain. Chem. Eng.* **2018**, *6*, 633-641.

15. Liu, B.; Liu, Y.; Chen, H.; Yang, M.; Li, H. MnO_2 Nanostructures Deposited on Graphene-Like Porous Carbon Nanosheets for High-Rate Performance and High-Energy Density Asymmetric Supercapacitors. *ACS Sustain. Chem. Eng.* **2019**, *7*, 3101-3110.

16. He, F.; Li, K.; Cong, S.; Yuan, H.; Wang, X.; Wu, B.; Zhang, R.; Chu, J.; Gong, M.; Xiong, S.; Wu, Y.; Zhou, A. Design and Synthesis of N-Doped Carbon Skeleton Assembled by Carbon Nanotubes and Graphene as a High-Performance Electrode Material for Supercapacitors. *ACS Appl. Energy Mater.* **2021**, *4*, 7731-7742.

17. Liang, H.; Xia, C.; Jiang, Q.; Gandi, A. N.; Schwingenschlögl, U.; Alshareef, H. N. Low temperature synthesis of ternary metal phosphides using plasma for asymmetric supercapacitors. *Nano Energy* **2017**, *35*, 331-340.

18. Lalwani, S.; Marichi, R. B.; Mishra, M.; Gupta, G.; Singh, G.; Sharma, R. K. Edge enriched cobalt ferrite nanorods for symmetric/asymmetric supercapacitive charge storage. *Electrochim. Acta* **2018**, *283*, 708-717.

19. Zhao, Y.; Xu, Y.; Zeng, J.; Kong, B.; Geng, X.; Li, D.; Gao, X.; Liang, K.; Xu, L.; Lian, J. Low-crystalline mesoporous $CoFe_2O_4$/C composite with oxygen vacancies for high energy density asymmetric supercapacitors. *RSC Adv.* **2017**, *7*, 55513-55522.

20. Yue, L.; Zhang, S.; Zhao, H.; Feng, Y.; Wang, M.; An, L.; Zhang, X.; Mi, J. One-pot synthesis $CoFe_2O_4$/CNTs composite for asymmetric supercapacitor electrode. *Solid State Ion.* **2019**, *329*, 15-24.

21. Gao, X.; Bi, J.; Wang, W.; Liu, H.; Chen, Y.; Hao, X.; Sun, X.; Liu, R. Morphology-controllable synthesis of $NiFe_2O_4$ growing on graphene nanosheets as advanced electrode material for high performance supercapacitors. *J. Alloys Compd.* **2020**, *826*, 154088.

22. Ouyang, Y.; Xia, X.; Ye, H.; Wang, L.; Jiao, X.; Lei, W.; Hao, Q. Three-dimensional hierarchical structure ZnO@C@NiO on carbon cloth for asymmetric supercapacitor with enhanced cycle stability. *ACS Appl. Mater. Interfaces* **2018**, *10*, 3549-3561.

23. Makkar, P.; Ghosh, N. N. Facile synthesis of $MnFe_2O_4$ hollow sphere-reduced graphene oxide nanocomposites as electrode materials for all-solid-state flexible high-performance asymmetric supercapacitors. *ACS Appl. Energy Mater.* **2020**, *3*, 2653-2664.

24. Makkar, P.; Ghosh N. N., High-Performance All-Solid-State Flexible Asymmetric Supercapacitor Device Based on a Ag-Ni Nanoparticle-Decorated Reduced Graphene Oxide Nanocomposite as an Advanced Cathode Material. *Ind. Eng. Chem. Res.* **2021**, *60*, 1666-1674.

25. Makkar, P.; Gogoi, D.; Roy, D.; Ghosh, N. N. Dual-Purpose $CuFe_2O_4$-rGO-Based Nanocomposite for Asymmetric Flexible Supercapacitors and Catalytic Reduction of Nitroaromatic Derivatives. *ACS Omega* **2021**, *6*, 28718-28728.

26. Makkar, P.; Ghosh, N. N. Snowflake-Like Dendritic CoNi Alloy-rGO Nanocomposite as a Cathode Electrode Material for an All-Solid-State Flexible Asymmetric High-Performance Supercapacitor Device. *ACS Omega* **2020**, *5*, 10572-10580.